

COMPACT MARX GENERATOR TRIGGERING

Jerald Parker, et al.

10 June 2022

Technical Paper

Approved for public release; distribution is unlimited. Public Affairs release approval 2022-3235.



**AIR FORCE RESEARCH LABORATORY
Directed Energy Directorate
3550 Aberdeen Ave SE
AIR FORCE MATERIEL COMMAND
KIRTLAND AIR FORCE BASE, NM 87117-5776**

NOTICE AND SIGNATURE PAGE

Using Government drawings, specifications, or other data included in this document for any purpose other than Government procurement does not in any way obligate the U.S. Government. The fact that the Government formulated or supplied the drawings, specifications, or other data does not license the holder or any other person or corporation; or convey any rights or permission to manufacture, use, or sell any patented invention that may relate to them.

This report was cleared for public release by AFRL/PA and is available to the general public, including foreign nationals. Copies may be obtained from the Defense Technical Information Center (DTIC) (<http://www.dtic.mil>).

AFRL-RD-PS-TP-2022-0014 HAS BEEN REVIEWED AND IS APPROVED FOR PUBLICATION IN ACCORDANCE WITH ASSIGNED DISTRIBUTION STATEMENT.

SCHROCK.JAMES.
ALAN.1394227303

Digitally signed by
SCHROCK.JAMES.ALAN.1394227303
Date: 2022.10.31 11:46:20 -06'00'

JAMES SCHROCK, DR-III
Senior Electronics Engineer, AFRL/RDHP

LANGDON.STEPH
EN.L.1232187065

Digitally signed by
LANGDON.STEPHEN.L.123218706
5
Date: 2022.10.31 12:33:55 -06'00'

STEPHEN LANGDON, DR-III
Branch Chief, AFRL/RDHP

This report is published in the interest of scientific and technical information exchange, and its publication does not constitute the Government's approval or disapproval of its ideas or findings.

TABLE OF CONTENTS

LIST OF FIGURES	ii
1.0 INTRODUCTION.....	1
2.0 MARX TRIGGERING SPICE CALCULATIONS.....	1
2.1 Preliminary Triggering Calculations	2
2.2 Trigger Resistor Methodology Comparisons	3
2.3 Additional Trigger Chain Analysis	5
3.0 ENHANCED MARX TRIGGERING DISCUSSION	7
3.1 Trigger Resistor Considerations.....	8
3.2 Stray Capacitance Considerations	9
3.3 Electrode Spacing Considerations.....	9
4.0 CONCLUSION	9
DISTRIBUTION LIST.....	10

LIST OF FIGURES

Figure 1: Simulated changes in the anode and cathode voltages with respect to ground.....	2
Figure 2: Standard trigger chain circuit (left). The modified circuit with the trigger pin of SG2 tied directly to ground (right).....	3
Figure 3: Simulated electrode voltages for SG2 for the two trigger configuration shown in Figure 3.	4
Figure 4: Simulated voltage difference between trigger pin and cathode: the “triggering” voltage.	5
Figure 5: The circuit configurations used to investigate the electrode voltages for SG3.....	6
Figure 6: Simulated electrode voltages on SG3 when SG1 and SG2 are triggered.....	7
Figure 7: Simulated voltage difference between trigger pin and cathode, the “triggering” voltage, for two trigger configurations.	7
Figure 8: The suggested trigger circuit configuration for the next generation compact Marx generator: single stage direct trigger, with alternating resistive back coupling to ground.	8

1.0 INTRODUCTION

A new compact Marx generator is being designed for use by the AFRL Directed Energy Directorate, High Power Electromagnetics Division. This memo presents trigger analysis leading to the recommendation of configuring the trigger circuit into a dual-branch resistive back-coupling topology. The recommendation is based upon modeling calculations performed with SPICE circuit modeling code. A summary of the calculations is presented, and a recommended circuit configuration and thoughts on improving Marx reliability are provided.

2.0 MARX TRIGGERING SPICE CALCULATIONS

The Marx undergoing development is a bipolar charged (+/-) device that is configured as six spark gap switches, five +/- charged capacitors and two half-voltage capacitors charged either +/- at opposite ends of the Marx. The half-voltage capacitors are implemented with twice the capacitance of the fully charged capacitors to maintain equal charge distribution throughout the Marx, and to prevent voltage reversal of the half-charge stages during Marx discharge. The utilization of the half-voltage capacitor stages enables the deletion of the commonly implemented ground and output spark gaps. The deletion of the ground spark gap significantly improves overall Marx operational stability and reliability because it provides a direct ground reference and prevents excessive floating voltages from reaching back into the power supplies and trigger circuitry during Marx erection, especially during prefire events. The calculations performed and the resulting recommendations are applicable only to this proposed configuration.

The SPICE model developed for this calculation primarily addresses the voltages induced on the spark gap electrodes when one or more of the spark gaps is switched. The switched spark gaps are modeled with simple SPICE switches that are actuated at specified time(s). No attempt is made to model the actual voltage-induced triggering of the spark gaps.

Because the voltage distribution along the Marx generator is primarily determined by the internal capacitance between stages and the stray capacitance from each stage to ground, an effort was made to estimate these capacitances using the established physical dimensions of the proposed design. These capacitances were calculated based on the parasitics for closely packed 20 nF (+/- stage) and 40 nF (half stage) General Atomic double ended fast pulse capacitors, rail gap spark gap electrodes, and a 0.45 m diameter Marx containment vessel. The values used in the calculation are tabulated below. The accuracy of these estimates is unknown but they are probably within a factor of two of the correct values.

Stage – Stage Capacitance	17 pF
Stage – Ground Capacitance	4 to 5 pF
Trigger pin – Ground Capacitance	1 pF
Trigger pin – Electrode Capacitance	0.5 pF

These estimated capacitances are relatively small because this is a gas-insulated Marx. They would be at least two times larger in an oil insulated design.

2.1 Preliminary Triggering Calculations

Although the primary objective of the SPICE calculations is to examine the triggering behavior of the Marx, it is instructive to first examine the effects of switching the first spark gap, SG1, on the voltage distribution within the Marx. Figure 1 shows the voltage to ground of the anode and cathode electrodes for the five un-switched spark gaps. In the SPICE model, SG1 was arbitrarily closed at $t = 10$ ns. The initial charge voltages were established to be +50 kV and -50 kV for convenience, but the results can easily be scaled down for lower charge voltages.

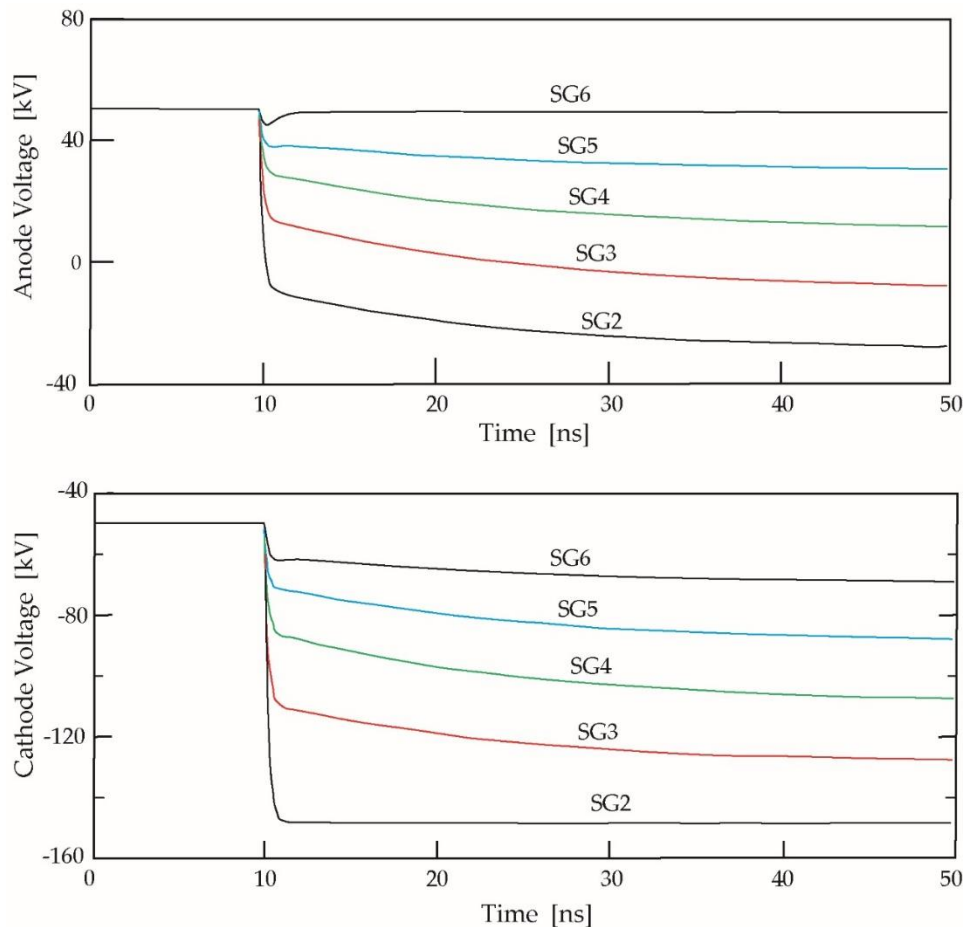


Figure 1: Simulated changes in the anode and cathode voltages with respect to ground.

On the plot of cathode voltages all of the electrode voltages are -50 kV prior to switching. As expected, the cathode voltage of SG2 falls abruptly to -150 kV as the first two capacitors are connected together. The inter-stage capacitance of the other stages act as a voltage divider so there is a smaller voltage change on the cathode electrode of each spark gap up the chain. The voltage division is not equal however. Charging the stray capacitance to ground of each stage reduces the voltage change on the upper electrodes.

The voltage changes on the anode electrodes are similarly distributed. The anode voltage change on the top gap, SG6, is very small since it is tied directly to ground through the top end capacitor and load resistor.

A noteworthy point that can be seen by examining the traces in Figure 1 concerns the voltage across the electrodes of SG2. At 1 ns after switching, the anode voltage has dropped to -8 kV and the cathode to -147 kV so that SG2 is now holding off 139 kV rather than the initial charge voltage of 100 kV . The dynamic changes in the spark gap electrode voltages suggest that subsequent triggering of the Marx stages may be complicated.

2.2 Trigger Resistor Methodology Comparisons

The first calculations performed to address Marx triggering were for the “conventional” trigger circuit configuration shown on the left of Fig. 2. In the model SG1 is a simple switch. There is no external pulse on the trigger input. The labels on SG1, i.e., A, K, T, identify the positively charged electrode (Anode), the negatively charged electrode (Kathode), and the Trigger pin for reference in the following discussions. The grounding resistor, R_g , is typically a large value, for example, $25\text{ k}\Omega$, which serves only to establish a ground potential of the trigger electrodes. The trigger coupling resistors are of lower resistance. In this calculation $R_T = 2\text{ k}\Omega$.

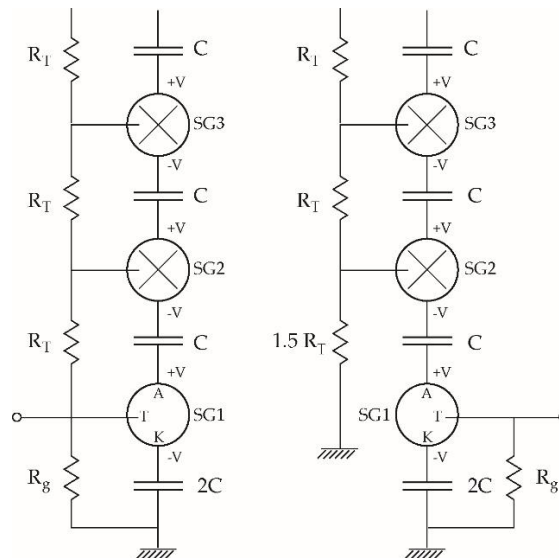


Figure 2: Standard trigger chain circuit (left). The modified circuit with the trigger pin of SG2 tied directly to ground (right).

Figure 3 shows the calculated SG2 electrode voltages for both configurations. As mentioned previously, the cathode voltage falls abruptly to -147 kV and the anode voltage to -8 kV . The anode and cathode voltage waveforms are the same for the two configurations.

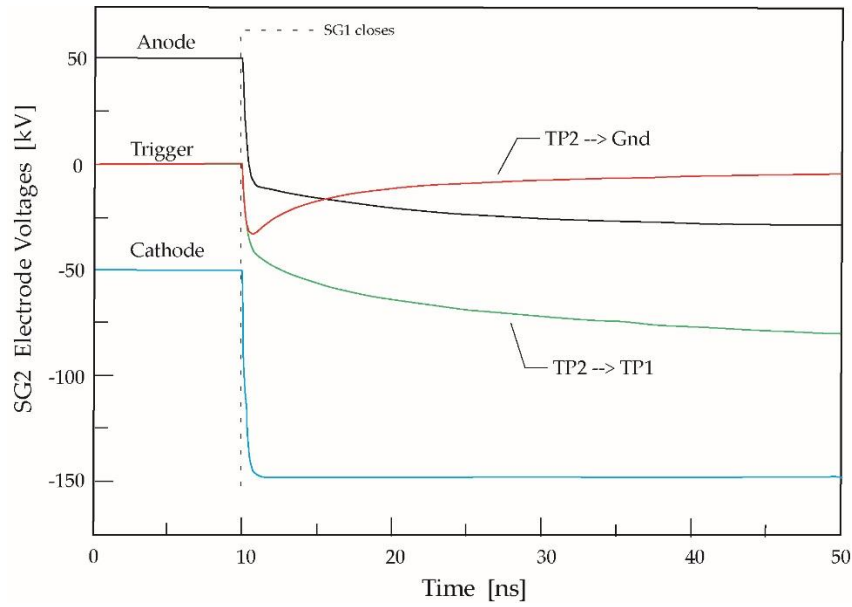


Figure 3: Simulated electrode voltages for SG2 for the two trigger configuration shown in Figure 3.

The green curve shows the calculated trigger pin voltage for the conventional configuration. Capacitive coupling to the trigger electrode causes its voltage to fall to -44 kV. The result of this capacitive coupling is to reduce the T-K voltage from 147 kV, if the trigger electrode was truly at ground potential, to 103 kV. Following the initial drop of the trigger electrode voltage, the voltage continues to fall as the stray capacitance of the trigger pin charges through R_T toward the -150 kV potential of the trigger pin of SG1.

The continued charging of the SG2 trigger pin toward -150 kV suggest that the alternative trigger configuration shown on the right of Fig. 2 might provide a better triggering voltage. The alternative circuit was modeled in SPICE. The value of the trigger pin resistor connecting SG2 to ground was increased to 3 kOhms due to the increase in its peak voltage from 100 kV to 150 kV. The electrode voltages for the modified trigger circuit are shown in Fig. 3 by the red curve. The trigger pin voltage, after an initial drop of -34 kV, immediately begins to rise as the trigger pin stray capacitance begins to discharge to ground.

Figure 4 compares the T-K voltage for these two cases. In both cases the voltage reaches ~ 100 kV in a fraction of a nanosecond. However, the voltage for the conventional trigger circuit then begins to decrease, reducing the probability of triggering SG2. In contrast, the T-K voltage for the modified trigger circuit continues to increase, reaching 120 kV at 1.8 ns and 130 kV at 4.7 ns. Although either waveform has the potential to trigger a discharge of SG2, the larger amplitude and longer duration generated by the modified trigger circuit certainly seems desirable.

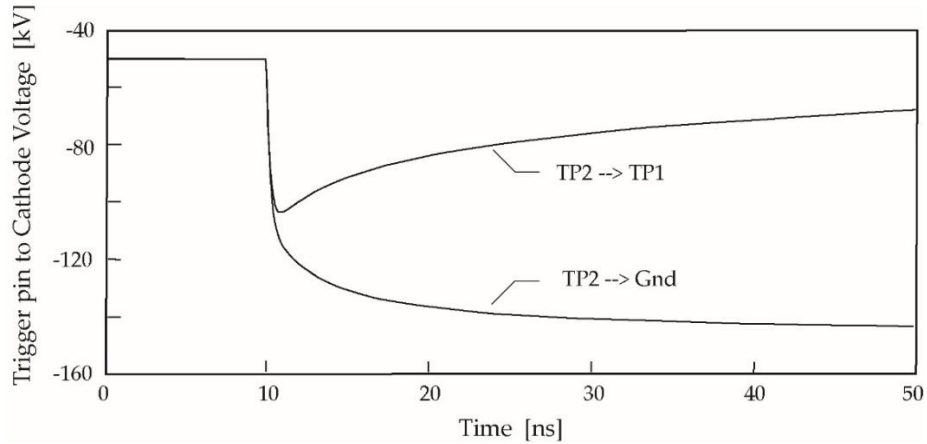


Figure 4: Simulated voltage difference between trigger pin and cathode: the “triggering” voltage.

2.3 Additional Trigger Chain Analysis

The beneficial effect calculated when the trigger pin of SG2 is connected to ground raises the obvious question, “Would changing the connection between SG3 and SG2 have a similar beneficial effect on the triggering of SG3?”

Answering this question requires modifying the SPICE model to simulate the closing of both SG1 and SG2. The modified SPICE circuit shown on the left in Figure 5 requires the addition of two more SPICE switches. When SG2 closes it has two effects on the circuit. First, the trigger pin of SG2 is shorted to the cathode (trigger pin breakdown) and then the anode and cathode are shorted together (gap closure). This behavior is modeled with switch S2, that shorts the trigger pin to the cathode, and switch S3 that connects anode to cathode. Both switches are activated at pre-set times. For this calculation switch S2 closes at $t = 12$ ns and switch S3 at $t = 14$ ns. There is no physical significance to these times, they were chosen to provide enough time between events so that waveform behavior could be examined.

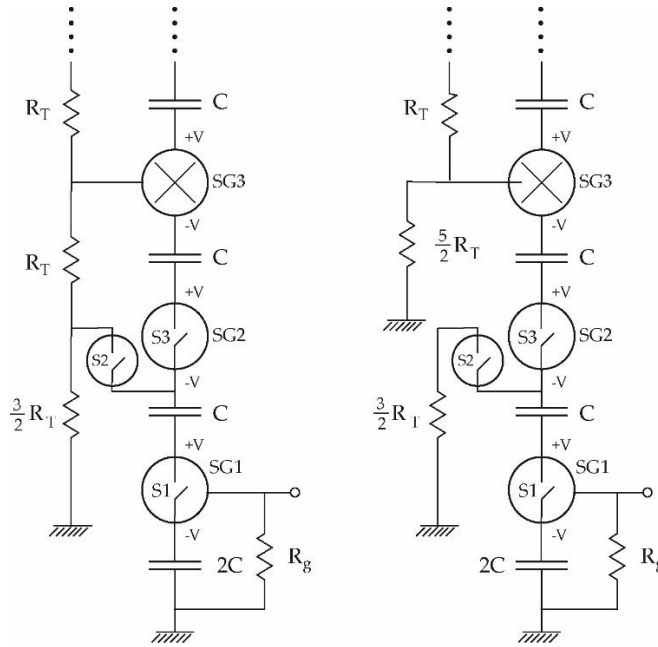


Figure 5: The circuit configurations used to investigate the electrode voltages for SG3.

Calculations of the electrode voltages for SG3 were performed for both of the configurations shown in Figure 5. For the remainder of this discussion the configuration on the left will be called “pin-to-pin” and the configuration on the right “pin-to-ground.” Figure 6 shows the calculated electrode voltages on SG3 for both configurations. Once again, the anode and cathode voltages are identical for both configurations. There are now two abrupt drops in both the anode and cathode voltages, first when SG1 closes and then when SG2 closes. The anode voltage falls immediately to -250 kV when SG2 closes as the cathode is now connected directly to the first three Marx capacitors in series.

The green curve, labeled TP3→TP2, shows the calculated trigger pin voltage for the pin-to-pin configuration. After SG1 closes the voltage falls to -25 kV due to capacitive coupling. When the trigger pin of SG2 shorts to the cathode of SG2, the trigger pin capacitance begins to charge through R_T toward -150 kV. When SG2 closes at 14 ns, the trigger pin voltage again falls abruptly due to capacitive coupling to -110 kV and then slowly toward -150 kV.

The red curve in Fig. 6 shows the trigger pin voltage for the pin-to-ground configuration. The trigger pin voltage waveform differs substantially. Following the closure of SG1, the voltage falls to -25 kV and then begins to increase as the trigger pin capacitance discharges through R_T to ground. Closure of SG2 causes a further drop to -55 kV after which the voltage begins increasing again as the pin capacitance continues to discharge to ground.

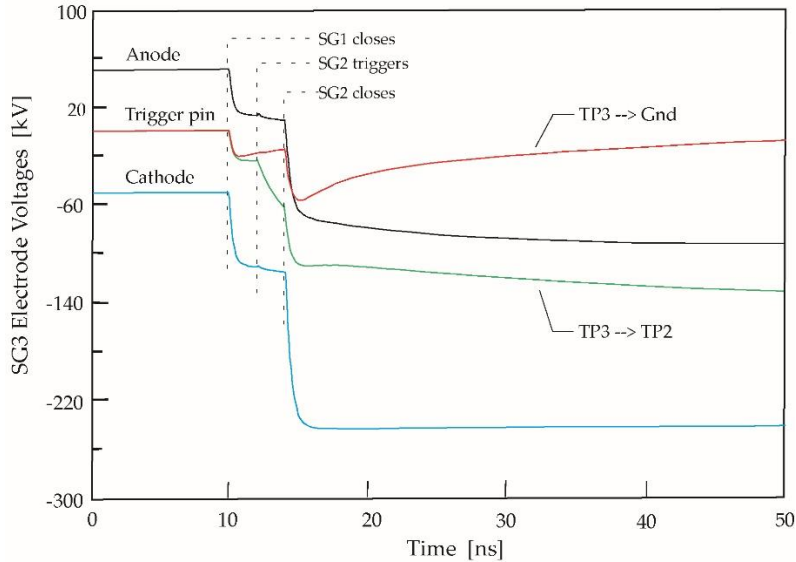


Figure 6: Simulated electrode voltages on SG3 when SG1 and SG2 are triggered.

Figure 7 compares the SG3 triggering voltage (T->K) for the two configurations. The improvement in this case is dramatic. While the pin-to-pin configuration provides an adequate trigger voltage of -132 kV about 2.5 ns after SG2 closes, the pin-to-ground configuration has already reached a voltage of -100 kV before SG2 even closes and then reaches -148 kV in less than 0.5 ns.

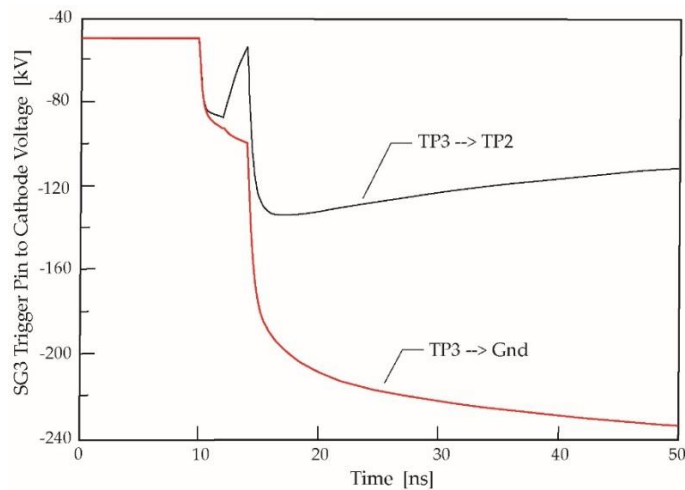


Figure 7: Simulated voltage difference between trigger pin and cathode, the “triggering” voltage, for two trigger configurations.

3.0 ENHANCED MARX TRIGGERING DISCUSSION

An obvious extension of the results presented in Section 2.0 would be to tie the trigger pins of all the higher spark gaps to ground to improve triggering. However, this is not a particularly practical idea. In addition to the complexity of running connections from the higher gaps to ground, the resistors would require very high voltage ratings.

Another option is suggested by the results of the calculations. Connecting the trigger pin of SG2 to SG1, $-V = 100$ kV, was detrimental; connecting the trigger pin of SG2 to ground, $-V = 150$ kV, was beneficial; connecting the trigger pin of SG3 to ground, $-V=250$ kV, gave great results. This suggests that skipping a stage, e.g., connecting the trigger pin of SG4 to SG2, $-V = 200$ kV, would provide improved triggering.

The resulting triggering circuit is shown in Figure 8. This is not a new idea. The dual trigger chain with resistive back coupling has been used since at least the '80s, primarily in multi-megavolt Marx generators with a large number of stages. The fact that this scheme has been used successfully is empirical evidence that it improves performance.

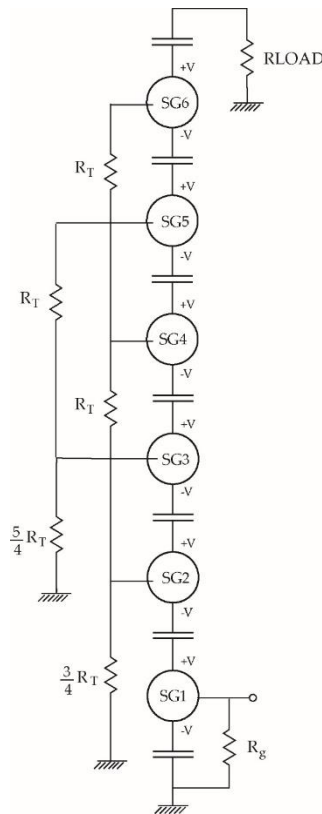


Figure 8: The suggested trigger circuit configuration for the next generation compact Marx generator: single stage direct trigger, with alternating resistive back coupling to ground.

The dual trigger chain configuration looks promising for the next generation Marx. In addition to improved triggering, it eliminates connection between the higher stages and the external trigger input, thereby providing some protection for the external trigger generator.

3.1 Trigger Resistor Considerations

Changing the trigger circuit to the dual chain configuration requires some care. The trigger bias resistors are subject to twice the voltage. In addition to the higher voltage rating, the resistance values should be increased by a factor of four to produce the same total current loss from the Marx output. In figure 8 the resistors for SG2 and SG3 are called out at 0.75 and 1.25 times the value of the upper stage resistors. This is not required. In practice they could all be the same resistance. It

is, however, important that the voltage rating of the resistor for SG3 be at least 2.5 times the stage voltage, or 1.25 times the rating of the other resistors in the trigger chain.

3.2 Stray Capacitance Considerations

The calculations presented above used estimated stray capacitance values. The details of the voltage waveforms for an as-built Marx will certainly differ to some degree. To the extent possible, the Marx components should be configured to increase the stray capacitance from the trigger pin circuitry to ground as this will hold the pin voltage more constant and improve triggering. Conversely, the stray capacitance from pin to pin should be minimized to avoid detrimental voltage changes from propagating from stage to stage.

3.3 Electrode Spacing Considerations

Finally, a thought for future consideration. As a Marx erects, the voltage across the open spark gaps increases rapidly because the total erected voltage is distributed only across the open gaps. For example, Fig. 6 shows the electrode voltages on SG3 as SG1 and SG2 close. In less than 2 ns after SG2 closes, the voltage between the anode and cathode of SG3 is 169 kV. Equal sharing of 600 kV among the four open gaps would predict $600/4 = 150$ kV, and this becomes true at late time. However, immediately after switching the new voltage distribution favors the lowest open gap. The voltage change on the higher stages is reduced by charging the stray capacitance from stage to ground. The increased voltage can be utilized to reduce the prefire risk by increasing the gap spacing of the higher stages. Reducing or eliminating prefires of the upper stages reduce the chance of a reverse erection. Reverse erections are particularly dangerous as they expose the trigger system and high voltage power supplies to damaging transient voltages.

There are obvious drawbacks to increasing the gap spacing, primarily an increase in the total inductance of the Marx. However, small changes, for example 30%, should have minimal impact. One would probably want to taper the increase; unchanged for SG1 and SG2, 15% for SG3 and SG4 and then 30 % for SG5 and SG6. Lots of possibilities and probably worth a try.

4.0 CONCLUSION

We presented a SPICE analysis of trigger schemes for a compact Marx generator with five bipolar charged capacitors and two half-voltage capacitors on either end. The SPICE investigation of a variety of trigger schemes displayed how the anode, cathode, and trigger voltages evolve with time during Marx erection, and how the trigger voltage evolution is a strong function of trigger resistor configuration. The SPICE modeling led to the recommendation of configuring the trigger resistors into a dual-branch resistive back-coupling topology. The simulations presented here demonstrate how this topology yields strong trigger bias drives, especially along the upper Marx stages.

DISTRIBUTION LIST

DTIC/OCP
8725 John J. Kingman Rd. Suite 0944
Ft Belvoir, VA 22060-6218 1 cy

AFRL/RVOP
Kirtland AFB, NM 87117-5776 1 cy

James Schrock
Official Record Copy
AFRL/RDHP 1 cy